

Velocity of plasma rotation in reflex discharge with thermionic cathode

© A.P. Oiler,^{1,2} G.D. Liziakin,¹ A.V. Gavrikov,^{1,2} V.P. Smirnov¹

¹ Joint Institute for High Temperatures of the Russian Academy of Sciences, Moscow, Russia

² Moscow Institute of Physics and Technology (National Research University), Dolgoprudny, Moscow Region, Russia
e-mail:andrey_oiler@mail.ru

Received May 18, 2022

Revised June 28, 2021

Accepted June 29, 2022

This work is devoted to determining the azimuthal ion rotation velocity in a reflex discharge with a thermionic cathode. For the experimental determination of the ion velocity, a Mach probe with directional particle collection was used. The Mach probe rotation velocity measurements are compared with the drift speed in crossed $\mathbf{E} \times \mathbf{B}$ fields, where the radial electric field is measured with an emissive probe. The rotation of the plasma was found to be predominantly due to this drift, corrected for centrifugal effects. One of the important results of the work is the determination of the ion temperature. The obtained value $T_i = 0.12$ eV, agrees with the ion temperature estimates in works with similar experimental conditions. A general parameter has been obtained that makes it possible to estimate the necessity to take into account centrifugal effects under given conditions.

Keywords: plasma, thermionic cathode, reflex discharge, ion rotation, crossed fields.

DOI: 10.21883/TP.2022.10.54359.139-22

Introduction

Reprocessing of spent nuclear fuel to close the nuclear fuel cycle is one of the challenges facing modern nuclear power. Plasma methods appear to be very promising, under them the mixture of heavy and light components is transferred to a plasma state and is further separated in electric and magnetic fields. The present paper is part of the studies carried out during the development of one of these methods on the LaPlaS setup [1,2].

The key issue for plasma methods based on the use of the T. Okawa mass filter [3] and the V.P. Smirnov separator [4] is the creation of a spatial distribution of the electrostatic potential with a given profile in magnetized plasma [5,6]. It is assumed that the particles of the separated substance will be entrained by the crossed $\mathbf{E} \times \mathbf{B}$ fields and separated in space according to their masses. Being in crossed electric and magnetic fields, the plasma begins to rotate in the azimuthal direction. The measurement of the plasma rotation speed will contribute to the understanding of the physical processes occurring in the reflex discharge, will make it possible to confirm the data obtained using the emission probe, and to determine the temperature of the ions.

In this paper we used a Mach probe to diagnose the velocity of charged particle flows. Such probe is used to study plasma in tokamaks [7], since there it is difficult to optically diagnose hydrogen atoms, the ion of which does not contain electrons for radiation emission. The Mach probe is the cheapest and easiest to manufacture probe for measuring charged particle flows [8], besides, it can measure ion flows in dusty plasma [9].

The simplest Mach probe consists of two conductive collectors separated by a dielectric. A potential negative relative to the surrounding plasma is applied to the collectors, due to which the probe collects ions in the ion saturation mode. From the collector, which is at „upstream“ side, the current I_{up} is collected, and the corresponding flow to the collector is called „upstream“. On the opposite collector („downstream“ side) current I_{down} is collected, the corresponding flow is „downstream“. The Mach number of the ion flow is determined from the semi-empirical formula [8,10–14]:

$$R = \frac{I_{\text{up}}}{I_{\text{down}}} = e^{KM}. \quad (1)$$

Here K is the calibration coefficient, the formula for which depends on the plasma magnetization and the mode of operation of the probe, and $M = v_d/c_s$ is the Mach number of the ion flow moving with a drift velocity v_d . The speed of sound is defined as $c_s = \sqrt{(T_i + T_e)/m_i}$.

The Mach probe has two modes of operation: magnetized and unmagnetized, which differ from each other by the ratios between the ion cyclotron radius r_c and the characteristic size of the probe collector r_p [13]. Currently, methods for measuring the Mach number of the ion flow for the magnetized probe are well developed [8]. These methods give close values for the calibration parameter K , and the values K are well defined both for ion flows along [7,13] and across the magnetic field [14]. In this case, it should be taken into account that a magnetic presheath [15] is formed near the collecting surface. In this region, an electric field normal to the surface is formed. With certain flow parameters, a situation may arise when the flow bypasses

the obstacle, and thus does not enter the collector. Thus, in the paper [16] the criteria were defined according to which it is determined whether the ion flow enters the surface of the Mach probe or not.

For the case of measuring the flow Mach number, when the probe is non-magnetized, there is no generally accepted approach to determine the calibration coefficient, and the discussion remains open [8]. Different theories offer their own values for the calibration coefficient [10–12,17], and some even use a formula for $R(M)$ [8, which differs from equation (1), 17]. As for the magnetic presheath, then for a unmagnetized probe the conditions when the particle enter the surface differ from the case of the magnetized probe. This is due to the fact that the problem of determining the particles dynamics in the vicinity of the collecting surface of the probe cannot be solved within the framework of the MHD approach and requires additional analysis, for example, within the framework of the PIC method [11].

It is also necessary to separate the different orientations of the flow with respect to the magnetic field. The leading [8,12,18] theory describing measurements of the ion flow co-directional with the magnetic field in the unmagnetized mode of the probe remains Hutchinson's theory [11], based on PIC-simulation and confirmed by a number of experiments [12,19,20].

Measurements of the ion flow velocity across the magnetic field are described by the theory of Hudis and Lidsky [10]. According to this theory the calibration factor is defined as

$$K = 4\sqrt{T_i/T_e}. \quad (2)$$

Note that this theory can only be applied to a narrow slit probe configuration (Directional Langmuir Probe) (DLP) configuration only. In this case, the conditions for the ratio of the temperature of ions and electrons $T_i \ll T_e$, as well as for the ratio of the Debye radius and probe size $30\lambda_D < r_p$ must be satisfied. The formation of the magnetic presheath, most likely, does not occur in such probe when measuring the transverse flow. This is due to the fact that the electrons do not enter the surface of the probe.

The main objective of this paper was to obtain the radial profile of the azimuthal rotation of the plasma of the reflex discharge with a thermionic cathode. According to estimates, the plasma of such discharge is magnetized, and the cyclotron radius of argon ions is several centimeters. Therefore, it is advisable to use the probe in the unmagnetized mode.

1. Description of the experimental setup

The diagram of the LaPlaS experimental setup is illustrated in Fig. 1. The vacuum chamber is 2.3 m long and has internal diameter of 86 cm. Two types of discharge can be ignited in the setup — radio-frequency and reflex. The first is ignited using an antenna wound around a dielectric cylinder. This cylinder is pressed by two earthed diaphragm flanges with an inner diameter of 500 mm. In the present

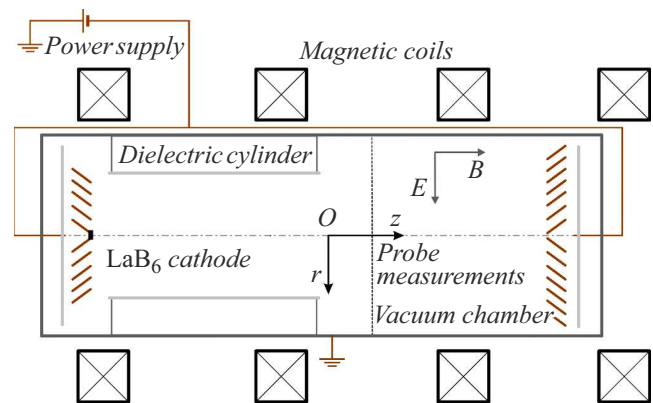


Figure 1. Block diagram of LaPlaS setup.

paper, the radio-frequency discharge was not used. An axial quasi-homogeneous magnetic field 1400 Gs is created by four coils, through which a current 900 A flows.

Electrodes are located at the ends of the chamber. Each of the electrodes occupies an area of 5 cm along the radius. Three internal electrodes are short-circuited at each end, and voltage of -550 V is applied to them (outer radius 15 cm). The fourth and fifth electrodes are under floating potential. The reflex discharge is ignited between the end cathodes and the cylindrical surface of the vacuum chamber, which is the anode. The discharge current is about 10 A. The radius of the plasma column is 25 cm. In such discharge a stationary radial electric field is formed, directed towards the chamber axis. A heated thermionic cell made of LaB₆ is installed on one of the ends. The limiting residual pressure is in the range $(5-8) \cdot 10^{-5}$ Torr. In the operating mode argon is filled into the chamber, and inleakage of 3.5 SCCM (Standard Cubic Centimeters per Minute) is maintained. The neutral gas pressure in this case is $3 \cdot 10^{-4}$ Torr.

The plasma potential is measured by an emissive probe, and the electron temperature and plasma density are measured by a double probe. The emissive probe, the double probe, and the Mach probe are introduced into the chamber radially at axial distance $z = 10$ cm from the central transverse plane (Fig. 1). The electron temperature is 5–10 eV, the plasma density is about 10^{11} cm⁻³, respectively, the degree of ionization is about 0.01.

2. Description of probe measurement system

The geometric dimensions of the Mach probe are shown in Fig. 2. The base of the probe consists of a ceramic (corundum) rod 15 cm long and 7 mm in diameter with 4 channels ~ 1 mm in diameter. These channels contain molybdenum wires 0.8 mm in diameter, which are collectors of the Mach probe. In the side surface of the rod 4 slots 1 mm wide and ~ 6 mm long are made, through which the ion flow is captured. The slot is 2 mm deep, so

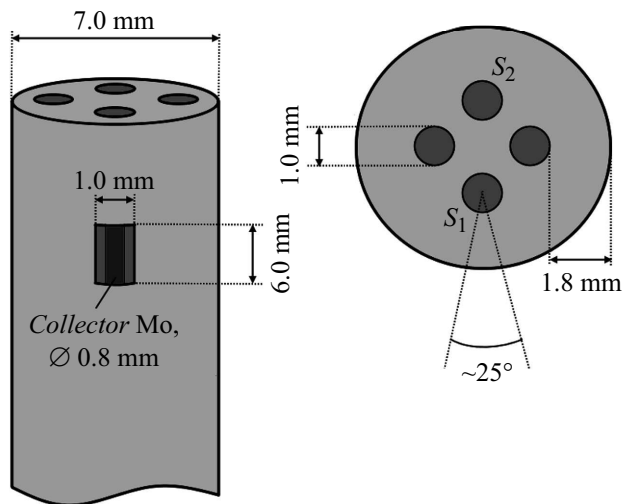


Figure 2. DLP diagram of Mach probe.

the ion collection angle is about 25° . This allows this probe configuration to be considered a DLP type. The channels are not closed from the end, however, the collectors are recessed to a depth of 5 mm from the edge, and there is no direct contact with the plasma. It is believed that the radial flow of ions across the magnetic field, caused by collisions with a neutral gas, is significantly less than the azimuthal one, in addition, the end area of the collector wire ($\sim 0.5 \text{ mm}^2$) is much smaller than the collecting area of collector ($\sim 4.8 \text{ mm}^2$), and therefore the radial flow does not introduce significant measurement errors.

Because the hole sizes may be different, the collecting areas on opposite sides of the probe may differ. Therefore, to obtain correct data, it is necessary to average the current values from opposite collectors. That is, first use collector with effective area S_1 as „upstream“, and S_2 — as „downstream“. Then, the probe rotates around its axis by 180° , and the collectors change places. Then already collector with area S_2 is used as „upstream“. Let us justify the correctness of this procedure. Let the effective areas of collectors are S_1 and S_2 . Then the currents ratio can be written as

$$R = \frac{I_{\text{up}}^{(0)} + I_{\text{up}}^{(180)}}{I_{\text{down}}^{(0)} + I_{\text{down}}^{(180)}} = \frac{j_{\text{up}}S_1 + j_{\text{up}}S_2}{j_{\text{down}}S_2 + j_{\text{down}}S_1} = \frac{j_{\text{up}}}{j_{\text{down}}} = e^{KM}.$$

This formula takes into account that equation (1), introduced for collectors with the same area, refers primarily to the ratio of the ion current densities j_{up} and j_{down} , not to the currents themselves. You can also find the necessary condition for the correctness of the obtained current values:

$$\frac{I_{\text{down}}^{(180)}}{I_{\text{down}}^{(0)}} = \frac{S_2}{S_1} = \frac{I_{\text{up}}^{(0)}}{I_{\text{up}}^{(180)}} \implies \eta = \frac{I_{\text{up}}^{(0)} I_{\text{down}}^{(0)}}{I_{\text{up}}^{(180)} I_{\text{down}}^{(180)}} = 1.$$

It follows that the product of currents from opposite collectors before ($I_{\text{up}}^{(0)}$ and $I_{\text{down}}^{(0)}$) and after rotation by 180°

($I_{\text{up}}^{(180)}$ and $I_{\text{down}}^{(180)}$) should be preserved. Thus, according to the number η it is possible to cut off experimental points, which obviously cannot be taken into account when processing experiments. Such experimental points can appear upon a significant change in the discharge mode during the turn or when the probe insulator is dusted with cathode material, which leads to an increase in the ion collection area. If $|1 - \eta| \ll 1$, then the experimental point can be included in the analysis. Another indicator, that the measurements are incorrect, is a sharp drop in the resistance between the probe channels, which occurs when the dielectric surface of the probe is heavily dusted. Then the estimation of the effective collection area is not possible.

To determine the voltage that must be applied to ensure that the probe is in saturation mode, the current-voltage characteristics (CVC) were obtained at various positions of the probe inside the chamber (Fig. 3). It can be seen in Fig. 3 that as the chamber axis is approached (decreasing of the radial coordinate), the exponential part of the CVC becomes wider both along the voltage axis and along the current axis. This is due to increasing of the plasma potential fluctuations. The minimum negative drift relative to the floating plasma potential (about 300 V for the radial coordinate $r = 5 \text{ cm}$), at which the probe is saturated over the entire measurement range, is 100 V.

Fig. 4 shows the schematic diagram of Mach probe measurements. The circuit consists of four identical parts, each of which is designed to receive signal from its own probe channel. Each channel is capable of switching between two modes: saturation current measurement mode and floating potential measurement mode. First, the floating potential is measured, then 100 V is subtracted from it to switch the probe to ion saturation. The first mode is the main one for the Mach probe, and it can be used to determine the ion flow rate. In the second mode, the floating potential in the measurement area is determined.

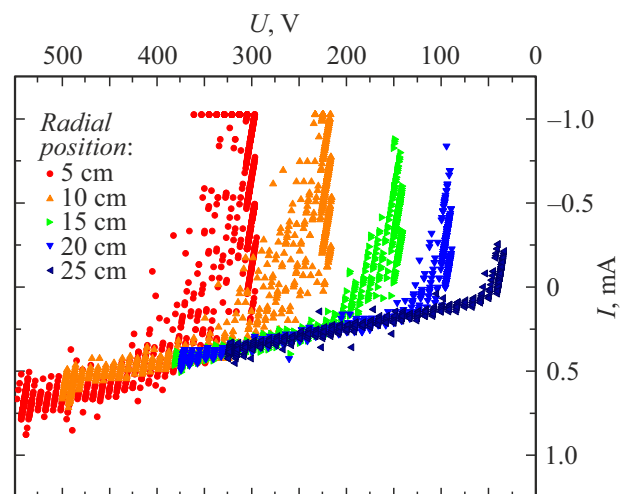


Figure 3. Ionic branches of CVC of Mach probe in various radial coordinates.

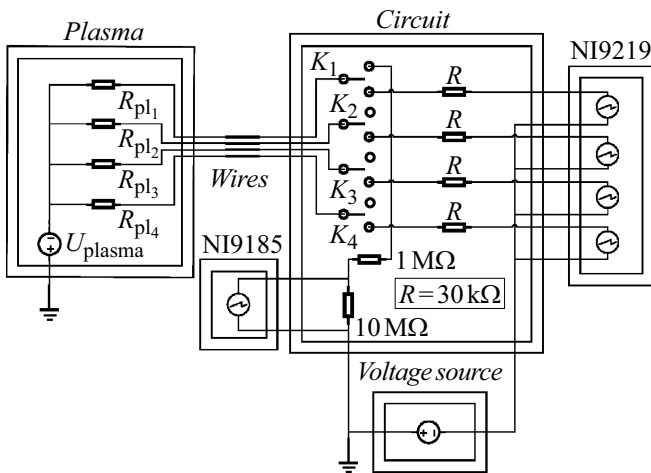


Figure 4. Schematic diagram of Mach probe measurements.

After the K_i switch in the current measurement mode the signal goes to the resistance $30\text{ k}\Omega$. The main function of this resistance is to protect the circuit from short circuit. Without it, in case of unintentional earthing of the probe channel, the voltage between the channels will be hundreds of volts, which can lead to failure of the measuring equipment. Then the current flows through the NI9219 module (24 digits, 100 measurements per second, relative measurement error 0.3%) [21], operating in the current measurement mode on the internal shunt. At room temperature the accuracy of these measurements is $0.75\text{ }\mu\text{A}$, which is negligibly small compared to collector current fluctuations.

3. Experimental results

In the course of the experimental study, the radial dependence of the ratio of the ion saturation currents R on the Mach probe was measured (Fig. 5, a). Here and below, the coordinate for radial profiles is measured from the axis of symmetry of the chamber. As can be seen from Fig. 5, a, that $\ln(R)$ is constant at the periphery, and decreases closer to the center of the discharge.

The plasma potential was measured with an emissive probe (Fig. 5, b). It can be seen in Fig. 5, b that the profile of the plasma potential is quasi-linear. The corresponding electric field strength is 14.5 V/cm . At the radial coordinate 6 cm , the potential reaches a value of about -275 V , and linear extrapolation suggests a value of -365 V on the discharge axis. At the boundary of the plasma column ($r = 25\text{ cm}$) the plasma potential becomes zero.

According to formula (1), the desired ion flow velocity is

$$v_d = \frac{c_s}{K} \ln R. \tag{3}$$

To determine the speed of sound and the calibration coefficient, a radial electron temperature profile was obtained using a double probe (Fig. 6, a).

The temperature profile has two regions, in each of which the electron temperature can be considered constant. In the first region from 5 to 13 cm , the electron temperature is $T_e \sim 9.5 \pm 1\text{ eV}$. This area is located opposite three short-circuited end electrodes, to which the discharge voltage is applied, their total radius is 15 cm (Fig. 1). The second region from 15 to 23 cm , in which the electron temperature is $T_i \sim 6 \pm 1\text{ eV}$, is located opposite the floating electrodes that are not interconnected. The main reason for this difference in the electron temperature obviously relates to the fact that electrons emitted from the electrode surface are accelerated in the cathode layer. Since the electrons are magnetized, longitudinal and transverse electron temperatures arise in this region. The Mach probe measures the azimuthal ion flow, which is directed across the magnetic field, so to correctly determine the speed of sound in the transverse direction, it is necessary to use the transverse electron temperature. An upper estimate for the transverse temperature can be the values obtained in the region opposite the floating electrodes.

According to expression (3), at constant temperature of electrons and ions, the ion rotation speed is directly proportional to $\ln(R)$. Then, as can be seen from Fig. 5, a, at the periphery the rotation speed is almost constant, and closer to the center of the discharge it begins to decrease.

The double probe also measured the radial plasma density profile (Fig. 6, b). In the center of the vacuum chamber up to 7 cm along the radius, there is a certain concentration gradient. Further, the gradient decreases, and in the region from 7 to 20 cm the concentration reaches a plateau. Closer to the edge of the plasma column the electron concentration drops, and the concentration gradient arises again.

4. Drift velocity in centrally symmetric field

In the planar case of homogeneous, crossed $\mathbf{E} \times \mathbf{B}$ fields, not considering collisions and concentration gradient, the drift velocity of the charged particle is equal to

$$v_d = \frac{E}{B}. \tag{4}$$

Let us calculate the drift velocity for the case of centrally symmetric field in the presence of collisions and a pressure gradient, and also find a parameter to assess the need to take into account the centrifugal effect. For this, we consider plasma in the hydrodynamic approximation. For the stationary case, we have a system of equations:

$$\begin{cases} (\mathbf{v}_i, \nabla) \mathbf{v}_i = -\frac{\nabla p_i}{\rho_i} + \frac{e(\mathbf{E} + \mathbf{v}_i \times \mathbf{B})}{m_i} - \\ v_{in}(\mathbf{v}_i - \mathbf{v}_n) - v_{ie}(\mathbf{v}_i - \mathbf{v}_e), \\ (\mathbf{v}_e, \nabla) \mathbf{v}_e = -\frac{\nabla p_e}{\rho_e} + \frac{e(\mathbf{E} + \mathbf{v}_e \times \mathbf{B})}{m_e} - \\ v_{en}(\mathbf{v}_e - \mathbf{v}_n) - v_{ei}(\mathbf{v}_e - \mathbf{v}_i), \\ (\mathbf{v}_n, \nabla) \mathbf{v}_n = -v_{ni}(\mathbf{v}_n - \mathbf{v}_i) - v_{ne}(\mathbf{v}_n - \mathbf{v}_e), \end{cases}$$

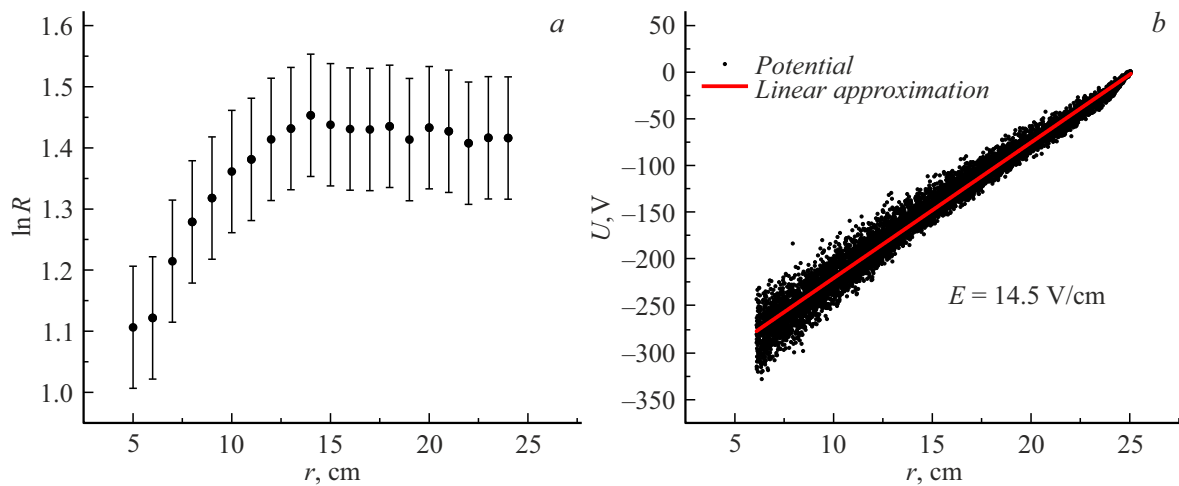


Figure 5. Radial dependence of $\ln(R)$ (a) and plasma potential (b).

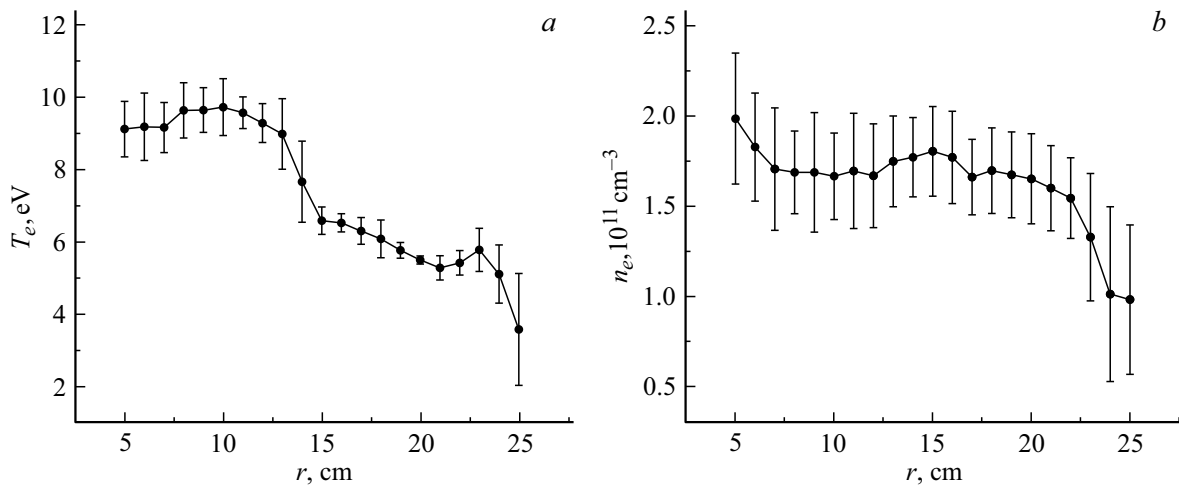


Figure 6. Radial profile: a — temperature, b — electron density.

where all ions, electrons and neutral atoms will be represented as liquids. Here \mathbf{v}_a , m_a are the velocity vector and the mass of the a -th plasma component; p_a , ρ_a are pressure and density of a -th fluid; e is elementary charge value; ν_{ab} is collision frequency of component a with component b .

In this consideration, we will neglect the following variables: viscous stresses (since at pressure of 0.3 mTorr the free molecular mode is realized), the velocity of the neutral liquid, the velocity of the directed motion of electrons (much less than the thermal motion), the frequency of collisions between charged particles (since plasma is weakly ionized). By virtue of the latter assumption, the electron and ionic liquids do not interact with each other, and therefore the equations describing them can be solved independently. Moreover, the equations have the same structure (up to the sign in front of the electron charge), and therefore the solution of the equation for ions is similar to the solution of the equation for electrons. Neglecting ion-ion and electron-electron collisions, we find that the concept of pressure is

already incorrect, since it implies interactions between fluid particles. Therefore, the term with the pressure gradient was also excluded from the equations.

Then, to consider stationary rotation in crossed \mathbf{E} and \mathbf{B} fields, we can write the stationary Euler equation for an ionic liquid:

$$(\mathbf{v}_i, \nabla)\mathbf{v}_i = e(\mathbf{E} + \mathbf{v}_i \times \mathbf{B})/m_i - \nu_{in}\mathbf{v}_i. \quad (5)$$

The projections of equation (5) in cylindrical coordinates look like this:

$$\begin{cases} v_{ir} \frac{dv_{ir}}{dr} - \frac{v_{i\varphi}^2}{r} = \frac{e}{m_i} (-E + v_{i\varphi}B) - \nu_{in}v_{ir}, \\ v_{ir} \frac{dv_{i\varphi}}{dr} - \frac{v_{i\varphi}v_{ir}}{r} = -\frac{e}{m_i} v_{ir}B - \nu_{in}v_{i\varphi}. \end{cases} \quad (6)$$

Let us first consider the solution of the system in the absence of collisions. Then the second equation takes the form

$$v_{ir} \left(\frac{dv_{i\varphi}}{dr} - \frac{v_{i\varphi}}{r} + \frac{e}{m_i} B \right) = 0. \quad (7)$$

It has the following solutions:

$$\begin{cases} v_{ir} = 0, \\ v_{i\varphi} = \frac{eB}{m_i} r \cdot \text{Ln}\left(\frac{r}{r_0}\right), \end{cases} \quad (8)$$

where r_0 is the integration constant. Since the flat case is limiting at $r \rightarrow \infty$ for the centrally symmetric case (zero curvature of the equipotential lines of the electric field), the expression for the azimuthal velocity in the collisionless mode must be reduced to expression (4). The second solution from (8) is not such, and therefore the physically correct solution of equation (7) is $v_{ir} = 0$. This is expected, since the radial motion in the magnetized plasma is due to particle collisions only. In view of this, the solution of the first equation (6) has the traditional form

$$v_{i\varphi} = \frac{eBr}{2m_i} \left(-1 + \sqrt{1 + \frac{4Em_i}{eB^2r}} \right). \quad (9)$$

Now let us solve system (6) taking into account collisions and the concentration gradient, assuming the first terms in the left sides of the equations to be negligible compared to the second ones. This assumption is valid, because, firstly, when the solution is substituted back into the system, these terms will turn out to be really small, and, secondly, in the collisionless limit, it will be reduced to expression (9). For short, let us denote v_0 as the drift velocity in crossed fields:

$$v_0 = \frac{E}{B}. \quad (10)$$

Let us ensure dimensionless of the equations (6) as follows:

$$u_{ir,i\varphi} = \frac{v_{ir,i\varphi}}{v_0}, \quad \rho = \frac{r}{r_c}, \quad r_c = \frac{v_0}{\Omega_c}, \quad \Omega_c = \frac{eB}{m_i}, \quad \chi = \frac{\Omega_c}{v_{in}}. \quad (11)$$

Here r_c and Ω_c are cyclotron radius and frequency respectively, χ is Hall parameter. Then we obtain

$$\begin{cases} -\frac{u_{i\varphi}^2}{\rho} = -1 + u_{i\varphi} - \frac{u_{ir}}{\chi}, \\ -\frac{u_{i\varphi}u_{ir}}{\rho} = -u_{ir} - \frac{u_{i\varphi}}{\chi}. \end{cases} \quad (12)$$

Let us express the radial velocity from the second equation of the system (12):

$$u_{ir} = \frac{1}{\chi} \frac{\rho u_{i\varphi}}{\rho + u_{i\varphi}}. \quad (13)$$

If we substitute the expression (13) into the first equation (12), then we get a cubic equation with respect to $u_{i\varphi}$:

$$\frac{u_{i\varphi}^3}{\rho^2} - u_{i\varphi} \left(1 + \frac{1}{\chi^2} + \frac{1}{\rho} \right) + 1 = 0. \quad (14)$$

We will assume that the rotation speed at an infinite distance from the center is not infinite. Then, proceeding

from (14), at infinity the velocity has the form $u_{i\varphi} = 1/K_d$, where $K_d = 1 + 1/\chi^2$ — drag factor, which is consistent with the papers [22,23], in which this rotation speed was obtained by neglecting the convective derivative in the left side (5) compared to the terms in the right side.

Three solutions of equation (14) have the following form:

$$\begin{aligned} u_{i\varphi}^{(n)} &= \sqrt{\frac{4}{3} \rho (1 + \rho K_d)} \\ &\times \cos \left[\frac{1}{3} \arctan \left(\sqrt{\frac{4}{27} \frac{(1 + \rho K_d)^3}{\rho} - 1} \right) + \frac{\pi + 2\pi n}{3} \right], \end{aligned} \quad (15)$$

where $n = 0, 1, 2$. At infinity, only the solution for $n = 0$ is finite, the other two tend to infinity. Returning to dimensional variables, we write the solution for $n = 0$ as follows:

$$\begin{aligned} v_{i\varphi} &= v_0 \sqrt{\frac{4}{3} \frac{\Omega_c r}{v_0} \left(1 + \frac{\Omega_c r}{v_0} K_d \right)} \\ &\times \cos \left[\frac{1}{3} \arctan \left(\sqrt{\frac{4}{27} \left(1 + \frac{\Omega_c r}{v_0} K_d \right)^3 - 1} \right) + \frac{\pi}{3} \right]. \end{aligned} \quad (16)$$

If we substitute the expression (15) with $n = 0$ into the expression (13) and return to the dimensional variables using (10) and (11), then we can make sure that the first term on the left side of the first equation of the system (6) is certainly much smaller than the second for any radial coordinate. When evaluating similar terms in the second equation, it turns out that the first term is less than the second one by at least 5 times at a distance $r > 2r_c$ from the discharge axis. Thus, the assumptions made earlier turned out to be correct. Moreover, if K_d tends to unity (the Hall parameter is infinite), then expression (16) reduces to expression (9) for $r > 0.5r_c$. For $r < 0.5r_c$, where the hydrodynamic approximation, strictly speaking, does not work, expression (16) tends to $v_{i\varphi} = \Omega_c r$.

Let us expand the expression (16) into a Taylor polynomial in $1/r$ with two terms

$$\begin{aligned} v_{i\varphi}(r) &= \frac{v_0(r)}{K_d} - \frac{v_0(r)^2}{\Omega_c r K_d^2} + O\left(\frac{1}{r^2}\right) \\ &= \frac{v_0(r)}{K_d} (1 - p(r)) + O\left(\frac{1}{r^2}\right), \end{aligned}$$

where $p = v_0/(\Omega_c r K_d)$. Then it appears that in regions where $|p(r)| \ll 1$, one can ignore the convective derivative in equation (5), and assume that the plasma rotation consists of a drift in crossed fields, corrected for the drag factor

$$v_{i\varphi}(r) = \frac{v_0(r)}{K_d} = \frac{1}{K_d} \frac{E}{B}.$$

When the parameter $p(r)$ becomes noticeably larger than 0.1, for a correct interpretation it is necessary to use formula (16). Fig. 7 shows the radial dependences of the parameter p for studies, in which the plasma rotation velocity was also studied using a Mach probe.

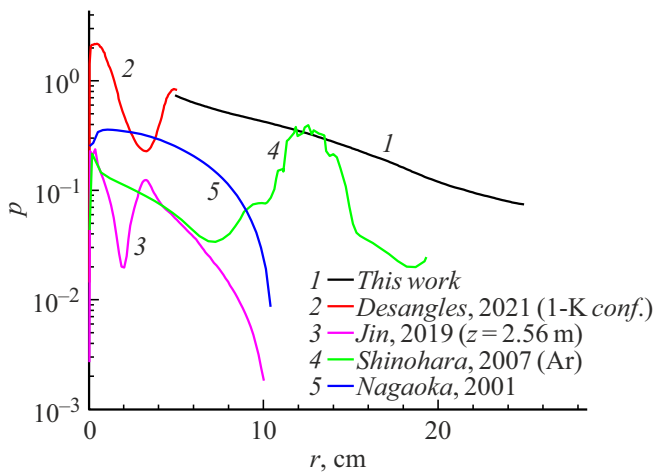


Figure 7. Radial dependencies of the parameter p for papers [22,24-26] and the present paper.

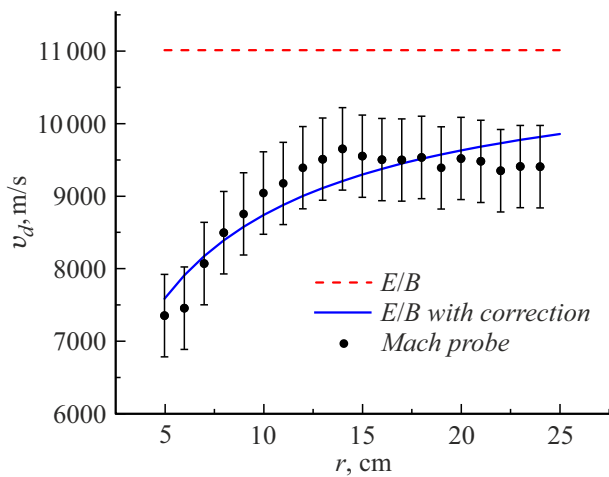


Figure 8. Radial dependence of the velocity of the azimuthal ion flow.

5. Discussion of results

It can be seen from Fig. 7 that when processing data from the Mach probe in this study, the centrifugal effects cannot be neglected. Fig. 8 shows the radial profile of the azimuthal plasma rotation speed. Black dots correspond to Mach probe measurements. The red straight line (in the online version) corresponds to the rotation speed calculated by formula (4), where the electric field was obtained from the radial profile of the plasma potential (Fig. 6, *a*). The blue color (in the online version) indicates the same data, but taking into account the part of the convective derivative in the equation (5) and calculated according to the expression (16).

Experimental data from the Mach probe were processed using the theory [10], i.e. coefficient K was calculated by formula (2). In this case, the ion temperature was chosen such that the experimental curve was as close as possible to the blue profile. The ion temperature was $T_i = 0.12$ eV. This

estimate of the ion temperature correlates with the values of the ion temperatures in papers with similar experimental conditions [25–27]. As a result, within the limits of error the experimentally determined profile of the azimuthal ion velocity coincides quite well with the profile obtained according to expression (16) using the experimental profiles of the plasma density and potential.

Conclusion

The analysis of the publications relating the topic of the Mach probe shows that there is a problem in determining the calibration coefficient in the unmagnetized probe mode. The discussion on this topic has not yet been closed, and the only work, which provides the theory most suitable for measuring the flow perpendicular to the magnetic field, is the work [10], according to which the interpretation of experimental measurements was carried out.

To confirm the experimental results, a theoretical model of plasma rotation with axial symmetry was developed. Based on the model, a criterion was formulated according to which it is possible to assess, in which cases centrifugal effects can be neglected.

Experimental measurements of the azimuthal rotation velocity of the reflex discharge plasma in the vacuum chamber of LaPlaS-1 plasma mass separator were carried out. The shape of the radial profile obtained using the Mach probe turned out to be the same as in the profile that was obtained using a theoretical model based on the plasma potential data obtained by the emissive probe. The ion temperature was $T_i = 0.12$ eV to ensure data coincidence within the experimental error. Note that the condition $T_e \gg T_i$, which is necessary for the possibility of using the theory, is satisfied, which indicates the correctness of the results obtained.

Funding

The study was supported by a grant from the Russian Science Foundation № 21-19-00716, <https://rscf.ru/en/project/21-19-00716/>

Conflict of interest

The authors declare that they have no conflict of interest.

References

- [1] G. Liziakin, N. Antonov, R. Usmanov, A. Melnikov, R. Timirkhanov, N. Vorona, V.S. Smirnov, A. Oiler, S. Kislenco, A. Gavrikov, V.P. Smirnov. *Plasma Phys. Contr. Fusion*, **63** (3), 032002 (2021). DOI: 10.1088/1361-6587/abd25e
- [2] G. Liziakin, N. Antonov, V.S. Smirnov, R. Timirkhanov, A. Oiler, R. Usmanov, A. Melnikov, N. Vorona, S. Kislenco, A. Gavrikov, V.P. Smirnov. *J. Phys. D: Appl. Phys.*, **54**, 414005 (2021). DOI: 10.1088/1361-6463/ac128e

- [3] T. Ohkawa, R.L. Miller. *Phys. Plasmas*, **9**, 5116 (2002). DOI: 10.1063/1.1523930
- [4] V.P. Smirnov, A.A. Samokhin, N.A. Vorona, A.V. Gavrikov. *Fizika plazmy*, **39** (523), 2013 (2006) (in Russian). DOI: 10.7868/s0367292113050107
- [5] G. Liziakin, A. Gavrikov, V. Smirnov. *Plasma Sourc. Sci. Technol.*, **29**, 015008 (2020). DOI: 10.1088/1361-6595/ab5ad5
- [6] G. Liziakin, A. Oiler, A. Gavrikov, N. Antonov, V. Smirnov. *J. Plasma Phys.*, **87** (4), 905870414 (2021). DOI: 10.1017/s0022377821000829
- [7] C.S. MacLatchy, C. Boucher, D.A. Poirier. *J. Gunn. Rev. Sci. Instrum.*, **63**, 3923 (1992). DOI: 10.1063/1.1143239
- [8] K.S. Chung. *Plasma Sourc. Sci. Technol.*, **21**, 063001 (2012). DOI: 10.1088/0963-0252/21/6/063001
- [9] S.A. Khrapak, B.A. Klumov, G.E. Morfill. *Phys. Plasmas*, **14**, 074702 (2007). DOI: 10.1063/1.2749259
- [10] M. Hudis, L.M. Lidsky. *J. Appl. Phys.*, **41**, 5011 (1970). DOI: 10.1063/1.1658578
- [11] I.H. Hutchinson. *Plasma Phys. Controll. Fusion*, **44** (9), 1953 (2002). DOI: 10.1088/0741-3335/44/9/313
- [12] T. Shikama, S. Kado, A. Okamoto, S. Kajita, S. Tanaka. *Phys. Plasmas*, **12**, 1 (2005). DOI: 10.1063/1.1872895
- [13] K.S. Chung, I.H. Hutchinson, B. Labombard, R.W. Conn. *Phys. Fluids B*, **1**, 2229 (1989). DOI: 10.1063/1.859039
- [14] J.P. Gunn, C. Boucher, P. Devynck, I. Đuran, K. Dya-bilin, J. Horaček, M. Hron, J. Stöckel, G. van Oost, H. van Goubergen, F. Žáček. *Phys. Plasmas*, **8**, 1995 (2001). DOI: 10.1063/1.1344560
- [15] P.C. Stangeby. *The Plasma Boundary of Magnetic Fusion Devices* (CRC Press, 2000)
- [16] I.H. Hutchinson. *Phys. Plasmas*, **15**, 123503 (2008).
- [17] L. Oksuz, N. Hershkowitz. *Plasma Sourc. Sci. Technol.*, **13**, 263 (2004). DOI: 10.1088/0963-0252/13/2/010
- [18] X. Zhang, D. Dandurand, T. Gray, M.R. Brown, V.S. Lukin. *Rev. Sci. Instrum.*, **82**, 033510 (2011). DOI: 10.1063/1.3559550
- [19] Y.S. Choi, H.J. Woo, K.S. Chung, M.J. Lee, D. Zimmerman, R. McWilliams. *Jpn. J. Appl. Phys., Part 1: Regular Papers and Short Notes and Review Papers*, **45**, 5945 (2006). DOI: 10.1143/JJAP.45.5945
- [20] C. Collins, M. Clark, C.M. Cooper, K. Flanagan, I.V. Khalzov, M.D. Nornberg, B. Seidlitz, J. Wallace, C.B. Forest. *Phys. Plasmas*, **21**, 042117 (2014). DOI: 10.1063/1.4872333
- [21] [Electronic source] Available at: <https://www.ni.com/docs/en-US/bundle/ni-9219-specs/page/overview.html>
- [22] V. Désangles, G. Bousselein, A. Poyé, N. Plihon. *J. Plasma Phys.*, **87** (3), 905870308 (2021). DOI: 10.1017/s0022377821000544
- [23] F.F. Chen. *Introduction to Plasma Physics and Controlled Fusion* (Springer International Publishing, Cham, 2016) DOI: 10.1007/978-3-319-22309-4
- [24] S. Jin, M.J. Poulos, B. van Compernelle, G.J. Morales. *Phys. Plasmas*, **26**, 022105 (2019). DOI: 10.1063/1.5063597
- [25] S. Shinohara, S. Horii. *Jpn. J. Appl. Phys., Part 1: Regular Papers and Short Notes and Review Papers*, **46**, 4276 (2007). DOI: 10.1143/JJAP.46.4276
- [26] K. Nagaoka, A. Okamoto, S. Yoshimura, M.Y. Tanaka. *J. Phys. Soc. Jpn.*, **70**, 131 (2001). DOI: 10.1143/JPSJ.70.131
- [27] S. Shinohara, N. Matsuoka, S. Matsuyama. *Phys. Plasmas*, **8**, 1154 (2001). DOI: 10.1063/1.1350663